

Article

# Study on Preparation and Properties of Sintered Brick from Multi-Source Solid Waste

Chen Guo <sup>1</sup>, Jiafeng Kong <sup>1</sup>, Zhenghua Wang <sup>2</sup>, Xiangbin Meng <sup>3</sup>, Yuchao Zhao <sup>3</sup>, Wenhao Wu <sup>1</sup>  
and Hongzhu Quan <sup>1,\*</sup>

<sup>1</sup> College of Civil Engineering & Architecture, Qingdao Agricultural University, Qingdao 266109, China

<sup>2</sup> Qingdao Sanxing Engineering Co., Ltd., Qingdao 266107, China

<sup>3</sup> Rizhao Lanshan District Ocean Development Co., Ltd., Rizhao 276800, China

\* Correspondence: quanhongzhu2006@qau.edu.cn

**Abstract:** The recycling of construction waste and the use of a new sintering process in the field of sintered bricks can greatly solve the problems of clay resource depletion, soil structure destruction, and high CO<sub>2</sub> emissions that always limit the development of the sintered brick field. The study was carried out using an orthogonal experiment to derive the optimal mix ratio for the preparation of sintered bricks, and subsequently, the sintered bricks were prepared using the optimal mix ratio. The experimental results show that the maximum compressive strength of construction waste sintered brick (MRB sintered brick) prepared using high-temperature sintering is 8.1 MPa, and the water absorption is 11. When the waste glass slag is mixed with 10%, it can show a better fluxing effect in the preparation of sintered bricks by mixing construction waste with waste glass slag (MGB sintered bricks), so that the MGB sintered bricks have a higher densification. The compressive strength is 32.9% higher and the water absorption is 3.5% lower than that of MRB sintered brick. MGS sintered bricks were prepared by mixing Yellow River sedimentary sand into MGB sintered bricks. The strength of MGS sintered bricks increased with the replacement rate of Yellow River sedimentary sand, and when the replacement rate of Yellow River sedimentary sand reached 16%, the strength of the MGS sintered bricks increased by 88.9%, and the water absorption rate was reduced by 4.6% compared with the MGB sintered bricks. The sintering mechanism had significant effects on the compressive strength, weathering resistance, and frost resistance of the sintered brick. The microwave sintering process has the characteristics of high efficiency, uniform heating, selective heating, and low thermal inertia, which can increase the compressive strength of MGS sintered brick by 4.6%, reduce the water absorption by 12.9%, shorten the sintering time by 43.6%, and improve the frost resistance.

**Keywords:** construction waste; sintered brick; Yellow River sedimentary sand; electric furnace sintering; microwave sintering



**Citation:** Guo, C.; Kong, J.; Wang, Z.; Meng, X.; Zhao, Y.; Wu, W.; Quan, H. Study on Preparation and Properties of Sintered Brick from Multi-Source Solid Waste. *Appl. Sci.* **2022**, *12*, 10181. <https://doi.org/10.3390/app121910181>

Academic Editor: Giuseppe Lacidogna

Received: 12 August 2022

Accepted: 27 September 2022

Published: 10 October 2022

**Publisher's Note:** MDPI stays neutral with regard to jurisdictional claims in published maps and institutional affiliations.



**Copyright:** © 2022 by the authors. Licensee MDPI, Basel, Switzerland. This article is an open access article distributed under the terms and conditions of the Creative Commons Attribution (CC BY) license (<https://creativecommons.org/licenses/by/4.0/>).

## 1. Introduction

Currently, the total amount of solid waste generated worldwide is about 17 billion tons per year, which is expected to increase to 27 billion tons by 2050 [1]; the annual new stockpile in China alone reaches nearly 2 billion tons [2], of which construction waste accounts for up to 92.2% [3]. Construction waste accounts for a relatively large stockpile and has good structural properties, hydrophilicity, high hardness, high water absorption, high permeability coefficient, and low crushing index [4–6], which have high advantages and feasibility for the preparation of sintered brick [7]. It can effectively alleviate the environmental pollution, ecological damage, and other safety problems of construction waste [8]. Waste glass is a common solid waste generated during construction and demolition. Mechanical grinding [9], chemical activation [10], and hydrothermal calcination [11] are the main methods used to improve the physicochemical properties of waste glass. The application of the improved waste glass slag to the preparation of sintered

bricks is beneficial for achieving resource utilization and for enhancing the performance of sintered bricks. The upper reaches of the Yellow River carry up to 80% of the total sediment in the Yellow River [12]. It is expected that in 2030, the water demand of the upper reaches of the Yellow River will continue to increase, leading to a further increase in the amount of sediment it carries [13]. The blending of sedimentary sand of the Yellow River into sintered brick can not only realize resource utilization, but also enhance various properties of sintered brick. The traditional sintered brick preparation process can no longer meet the development requirements of today's society. On the one hand, China is a large producer of sintered bricks. A large number of kilns in China have high energy consumption, low effective energy utilization rate, high treatment costs during production [14], and serious pollution of the surrounding air and soil by the generated exhaust gases [15,16]. On the other hand, a low-carbon strategy and low-carbon economy have become the development trends of the future industry. The structured development of the sintered brick industry is seriously inhibited. Sintered bricks are prepared using a microwave sintering process to achieve a clean and efficient process, which are advantageous for sintered brick production in terms of resources and environmental protection.

A summary of the previous studies is shown in Table 1. Among the various disposal methods of construction waste, Xiao et al. [17] found that the simple sorting and crushing of construction waste for the recycling and preparation of sintered bricks from recycled construction debris had advantages such as chemical composition compliance and perfect manufacturing equipment. Ma Wen et al. [18] demonstrated that the physical and mechanical properties of sintered bricks met the standard requirements of sintered bricks when the mud admixture was  $\leq 12\%$  and the firing temperature was  $1100\text{ }^{\circ}\text{C}$ . Sun et al. [19] blended fly ash into clay sintered bricks and modified the fly ash by exploring its effects on physical, mechanical, porosity, and environmental risks during the production process. The experiments showed that fly ash could be used in sintered brick production after washing to remove soluble salts, and all of the properties met the specification requirements. Dubale, M. et al. [20] sintered alumina abrasive wastes at different temperatures such as  $900\text{ }^{\circ}\text{C}$  and  $1100\text{ }^{\circ}\text{C}$ , and confirmed that the content of alumina and silica within the sintered brick could be enhanced, and that its mechanical properties improved after the incorporation of alumina abrasive wastes. Erdogmus et al. [21] prepared sintered brick from a mixture of water treatment sludge and sintered brick waste, and the sintered brick had excellent performance and low differentiation when 70–85% of the sludge was blended. Wang et al. [22] used waste glass slag instead of natural sand for concrete application to investigate the effect of contaminants in waste glass slag on concrete properties, and found that the effect of contaminants on concrete properties was negligible when 10% of the waste glass slag replaced natural sand. Cheng et al. [23] used waste glass as an aggregate to prepare asphalt micro-paving materials, and confirmed that the two-dimensional form of waste glass that was richer than basalt was abundant; with the increase of waste glass content, the waste glass improved the slip resistance of the mix to some extent. Fu et al. [24] prepared lightweight, high-strength porous ceramic materials with self-cleaning properties, stability, and superhydrophobicity by high-temperature sintering at  $1550\text{ }^{\circ}\text{C}$  using waste glass powder as raw material. Chen et al. [25] synthesized uranium tailings microcrystalline glass using microwave sintering at  $1200\text{ }^{\circ}\text{C}$ , and the cured samples exhibited a uniform and dense microstructure with suitable component parameters.

This study investigates the influence law of different sintering mechanisms on the performance of MRB sintered bricks to improve the controllability and stability of the sintering process. Additionally, the fluxing effect of waste glass slag on MGB sintered bricks, and the promotion effect of sintering mechanisms on mineral transformation to improve the mechanical properties and durability performance of MGB sintered bricks are analyzed. Furthermore, we analyze the effect of Yellow River sedimentary sand on the MGS sintered bricks under different sintering mechanisms. Finally, the formation of the skeletal structure of MGS sintered bricks under different sintering mechanisms was analyzed. By combining the microwave sintering process with sintered brick preparation

technology, the sintering quality and stability of MGS sintered bricks can be improved by adjusting and optimizing the temperature rise parameters.

**Table 1.** Summary of previous studies.

Authors	Types of Research Areas	Research Content
Xiao et al.	Construction waste	Preparation of sintered bricks from recycled construction debris.
Ma et al.	Construction waste	Preparation of sintered bricks using urban sludge as an admixture.
Sun et al.	Construction waste	Mixing fly ash into clay sintered bricks.
Dubale et al.	Construction waste	The alumina abrasive waste has been sintered at high temperatures to enhance the performance of the sintered brick.
Erdogmus et al.	Construction waste	Sintered bricks are prepared by mixing water treatment sludge and sintered brick waste.
Wang et al.	Waste glass	Using waste glass slag instead of natural sand in concrete applications.
Cheng et al.	Waste glass	Preparation of asphalt micro-paving materials by using waste glass as aggregates.
Fu et al.	Waste glass	The ceramic material is prepared using high-temperature sintering, with waste glass powder as raw material.
Chen et al.	Microwave sintering technology	Synthesis of uranium tailing microcrystalline glass using microwave sintering at 1200 °C.

The preparation of sintered bricks using construction solid waste is of great significance to improve the utilization rate of solid waste resources, and to alleviate the consumption of non-renewable resources such as clay, but this still needs further explorative research, mainly including:

(1) Further improvement of the utilization rate of sintered bricks for other solid wastes. Enhancement of the comprehensive utilization capacity of sintered bricks for solid waste can effectively alleviate the problems of raw material scarcity and environmental pollution.

(2) Improving the production efficiency of sintered bricks and achieving low energy consumption, high efficiency, and the green and batch production of sintered bricks.

## 2. Materials and Methods

### 2.1. Materials

The cementitious materials were construction waste (road work redevelopment, CHN), and its physical properties are shown in Table 2. Waste glass (remodeling area demolition, CHN) and Yellow River Sand (the lower section of the Yellow River in Gaoqing County, CHN) were used as supplementary cementitious materials, aiming to improve mechanical properties, and their physical properties are shown in Tables 3 and 4. The X-ray diffraction (XRD) analysis is shown in Figure 1. From the XRD analysis of construction waste and clay presented in Figure 1a, it can be seen that the intensities of diffraction peaks of the main components of the two clays are similar, the main phase of quartz (SiO<sub>2</sub>) is the main component, and the contents of MgO and CaO are slightly lower than those of clay, which can effectively avoid the problems of frost and lime burst for sintered brick. The chemical compositions of construction waste, waste glass slag, and Yellow River sand measured via X-ray fluorescence (XRF) are presented in Table 5. The mixing water is tap water, and its content was calculated using the mass of cementitious materials.

**Table 2.** Physical properties of construction waste.

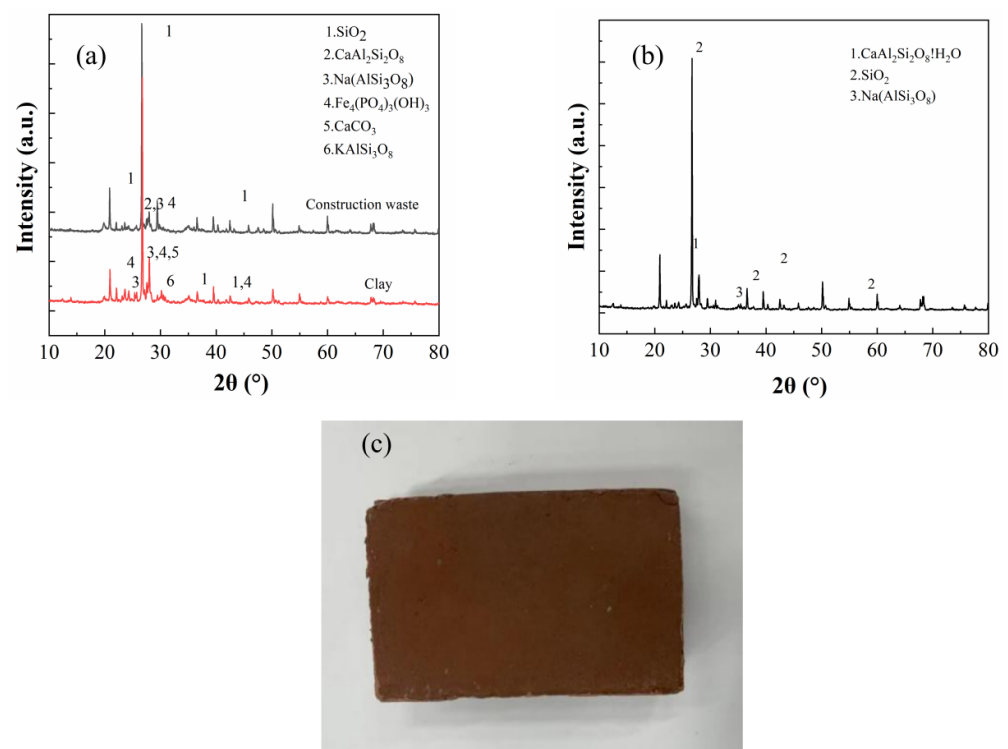
Type	Water Content/%	Water Absorption/%	Plasticity Index	Liquidity Index	Density/g × cm <sup>-3</sup>	
					Wet Density	Dry Density
Construction waste	5.5	8.5	16.0	0.5	1.8	1.7

**Table 3.** Physical properties of waste glass slag.

Type	Proportion	Melting Point/°C	Relative Density/g × cm <sup>-3</sup>
Waste glass slag	5.5	700–950	3.0

**Table 4.** Physical properties of Yellow River sand.

Type	Particle Grading/mm	Mud Content/%	Apparent Density/kg × m <sup>-3</sup>		Bulk Density /kg × m <sup>-3</sup>	Porosity /%	Water Absorption at Saturated Surface-Dry Basis /%
			Saturated Dry-Surface	Dry State			
Yellow River sand	5.5	2.1	2610	2630	1540	41	1.9

**Figure 1.** XRD analysis and prepared brick. (a) Construction waste and clay. (b) Yellow River sand. (c) Prepared brick.**Table 5.** XRF analysis results.

Type	SiO <sub>2</sub>	Al <sub>2</sub> O <sub>3</sub>	CaO	Fe <sub>2</sub> O <sub>3</sub>	SO <sub>3</sub>	MgO	Na <sub>2</sub> O	K <sub>2</sub> O	TiO <sub>2</sub>	ZrO <sub>2</sub>	LOI
Construction waste	57.4	17.3	6.1	4.0	0.2	1.8	2.5	3.6	0.6	–	6.5
Waste glass slag	64.3	13.2	9.5	4.4	0.2	1.4	3.3	1.8	1.1	0.2	0.6
Yellow River sand	66.5	12.8	7.7	4.4	0.1	2.4	2.0	2.8	1.0	–	0.3

## 2.2. Preparation Procedures and Design

The orthogonal experimental method was used to obtain the significance level, which includes the construction waste, waste glass slag, and Yellow River sand, respectively, as shown in Table 6. The raw materials under 0.3 mm were sieve-mixed with water for 90 s, and then aged for 48 h. Subsequently, the composite was pressed at 1–2 MPa to produce a raw brick. Finally, the raw brick was put into an electric furnace (BEQ-ZMF-1700C-18L,

Anhui BEQ Equipment Technology Co. Ltd., Heifei, China) and a microwave furnace (Kelangte, Qingdao, China) for roasting.

**Table 6.** Orthogonal test factor level table.

Construction Waste/% (Factor A)	Waste Glass Slag Content (kg/m <sup>3</sup> ) (B)	Content of the Yellow River Sand (%) (C)
45.0	6.0	8.0
50.0	8.0	12.0
55.0	10.0	16.0
	12.0	20.0
	14.0	24.0

Construction waste, waste glass slag, and Yellow River sedimentary sand were added to the cement net slurry mixer in that order, according to the matching ratio, and mixed evenly in a dry way; the aged material was mixed wet for 3 min after adding water, and the preparation was performed and tested for strength. The orthogonal experimental design and performance test results are shown in Table 7.

**Table 7.** Orthogonal experimental design and compressive strength test results.

No.	A	B	C	Content of Construction Waste (%)	Glass Slag Content (%)	Content of the Yellow River Sand (%)	Compressive Strength (MPa)
1	1	1	1	45.0	6.0	16.0	10.6
2	1	2	3	45.0	8.0	12.0	8.9
3	1	3	5	45.0	10.0	8.0	6.3
4	1	4	2	45.0	12.0	24.0	6.8
5	1	5	4	45.0	14.0	20.0	8.8
6	2	1	5	50.0	6.0	24.0	14.2
7	2	2	2	50.0	8.0	20.0	17.1
8	2	3	4	50.0	10.0	16.0	24.6
9	2	4	1	50.0	12.0	12.0	22.8
10	2	5	3	50.0	14.0	8.0	19.7
11	3	1	4	55.0	6.0	12.0	17.5
12	3	2	1	55.0	8.0	8.0	16.4
13	3	3	3	55.0	10.0	24.0	13.9
14	3	4	5	55.0	12.0	20.0	16.7
15	3	5	2	55.0	14.0	16.0	19.0

The extreme difference analysis of the effect of each factor on the compressive strength is shown in Table 8.

**Table 8.** Range analysis of influence of various factors on compressive strength.

Project	Compressive Strength (MPa)		
	A	B	C
Mean value T <sub>1j</sub>	8.3	14.1	14.1
Mean value T <sub>2j</sub>	19.7	14.1	16.4
Mean value T <sub>3j</sub>	16.7	14.9	18.1
Mean value T <sub>4j</sub>	–	15.4	14.2
Mean value T <sub>5j</sub>	–	15.8	11.6
Range value R <sub>j</sub>	11.4	1.7	6.5

As seen from Table 8,

(1) For factor A: When the amount of building residue gradually increases from 45% to 55%, the compressive strength of the sintered brick shows an obvious trend of first increasing and then decreasing. When the amount of building residue is too low, the clay content is low, and the combination between the particles is not sufficient to bring out the maximum cohesion.

(2) For factor B: When the amount of waste glass slag is increased from 6% to 14%, the strength of the sintered brick changes smoothly, the overall trend is gradually increased, and the average value of the sintered brick strength reaches the maximum when the amount of slag is 14%. At this time, glass slag acts as a co-solvent and plays a cementing role between the soil materials, thus improving the strength of the sintered brick. On the basis of the influence of glass slag on the durability of the sintered brick, the dose of glass slag used in this paper is 10%.

(3) For factor C: The strength of the sintered brick increases when the doping amount of Yellow River sedimentary sand increases from 8% to 24%. In total, 16% of Yellow River sedimentary sand doping is used in this paper to correct and optimize the particle size distribution. Additionally, when the doping of Yellow River sedimentary sand continues to increase, and the proportion of the clay particles of sintered brick decreases accordingly, which eventually leads to a decrease in the compressive strength of the sintered brick.

(4) The order of the range analysis of the influence of each factor on the compressive strength is: the amount of construction waste A > the amount of glass slag doping B > the amount of Yellow River sedimentary sand doping C.

In order to analyze the significance and difference of the effects of three factors on the data, this paper uses a three-factor ANOVA to further study the relationship between the amount of construction waste, waste glass slag doping, and Yellow River sedimentary sand doping on the compressive strength, and the results are shown in Table 9.

**Table 9.** Results of three-factor variance analysis.

Source of Variance	Square Sum	Df	Sean Square	F	p
Intercept	3324.193	1	3324.193	1207.121	0.000
Content of construction waste (%) (A)	349.561	2	174.781	63.468	0.001
Glass slag content (%) (B)	13.543	4	3.386	1.230	0.423
Content of the Yellow River sand (%) (C)	78.470	4	19.618	7.124	0.042
Residue	11.015	4	2.754	–	–

Table Note: Under the confidence interval of 95%,  $p < 0.05$  indicates significant effect.

From Table 9, it can be seen that: the amount of construction waste showed significance ( $F = 63.468, p = 0.001 < 0.05$ ), indicating that the main effect exists, and that the water content will have a differential relationship to the compressive strength. The glass slag substitution rate did not show significance ( $F = 1.230, p = 0.423 > 0.05$ ), indicating that the waste glass slag as a co-solvent with about 10% admixture does not have a significant differential relationship to the compressive strength. The Yellow River sediment sand substitution rate showed significance ( $F = 7.124, p = 0.042 < 0.05$ ), indicating that the main effect exists and that the Yellow River sediment sand substitution rate will have a differential relationship to the compressive strength. The results of the three-factor ANOVA were correlated with the results of the ANOVA, and the sum of squares confirmed that the amount of construction waste > the amount of Yellow River sedimentary sand blending > the amount of glass slag blending, and that the degree of influence of the three factors on the compressive strength of sintered brick was, in order, the amount of construction waste > the amount of Yellow River sedimentary sand blending > the amount of glass slag blending.

Combined with the experimental study, the main reasons for the three-factor ANOVA results and the extreme difference analysis results were analyzed as follows.

(1) Clay particles play a vital role in the sintered brick forming process, and when the amount of construction waste is increased from 45% to 50%, the content of clay particles increases, and the bricks possess a certain wet strength.

(2) Yellow River sedimentary sand has a substitution rate of 16% when the billet body forms a complete skeletal structure, but when the substitution rate continues to increase, it will lead to sintered brick strength reduction or even structural damage. This is due to the free water present around the saturated soil particles in the soil material at this time;

according to the gravitational effect of the electric field to encapsulate the strong binding water film, the aged material reflects a strong viscosity. In addition, the liquid phase in the mixture wraps and bonds the grains to enhance the densification of the waste sintered brick, thus making the waste sintered brick have higher strength and lower water absorption. When the substitution rate is greater than 20%, the content of the viscous particles decreases, and the structural stability of the waste sintered brick is damaged, resulting in a large number of cracks, which reduces the strength and increases the water absorption.

(3) A total of 10% of glass slag is incorporated to effectively reduce the firing temperature of sintered brick, play the effect of flux, and enhance the strength of sintered brick.

In summary, this paper adopts 50% of construction waste, 10% of glass slag admixture, and 16% of Yellow River sedimentary sand replacement rate as the matching ratio for subsequent research.

### 2.3. Testing Methods

#### 2.3.1. Compressive Strength Test

According to the test by the one-time molding method specified in the specification GB/T 2542-2012, "Masonry Wall Brick Experimental Method" [26], the sample brick was first cut from the middle, soaked in clean water for 20–30 min, and then placed on the iron net dripping for 20–30 min, and then a cement net paste of appropriate consistency was stirred, and the sample brick was evenly wrapped on the upper and lower surfaces and at the overlapping interface after the cuts were reversed and stacked. The slurry was wrapped evenly on the upper and lower surfaces and at the overlapping interface, as shown in Figure 2.

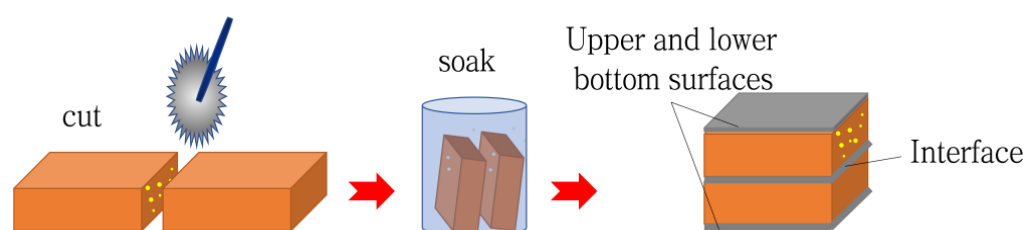


Figure 2. Preparation of compressive strength samples.

The test was carried out on the specimen bricks using a universal pressure tester, and the compressive strength of individual samples was calculated according to Equation (1).

$$R_p = \frac{p}{s} \tag{1}$$

$R_p$ —Compressive strength of a single sample, in MPa.

$p$ —Maximum breaking load, in N.

$s$ —Sample compressed area, unit  $\text{mm}^2$ .

In order to prevent errors in the test data of the individual test samples, the final results of compressive strength were calculated using the arithmetic mean of multiple samples, and in accordance with Equation (2).

$$\bar{R}_p = \frac{\sum_i^n R_{p,i}}{n} \tag{2}$$

$\bar{R}_p$ —Average value of compressive strength in MPa.

$n$ —The number of tested samples.

$R_{p,i}$ —Compressive strength of the  $i$ th sample, in MPa.

Multiple samples are required to calculate the standard deviation, which is calculated according to Equation (3). The calculation formula is as follows.

$$S = \left[ \frac{\sum_i^n (R_{p,i} - \bar{R}_p)^2}{n - 1} \right]^{1/2} \quad (3)$$

S—Standard deviation, MPa.

### 2.3.2. Weathering Resistance Test

Water absorption is a key factor affecting the performance of sintered brick, and is greatly influenced by the sintering method. In this paper, the water absorption rate at room temperature, and the 3 h boiling water absorption rate of the sample bricks were studied experimentally, and double specimens were prepared before the test, with 5 sintered bricks in each specimen. According to GB/T 2542-2012, “Masonry Wall Brick Test Method” [26], a quarter of the regular size of the sample brick was taken as the test specimen, and the specimen was firstly cleaned on the surface and dried in a blast drying oven at  $105 \pm 5$  °C to a constant weight, and the dry weight was weighed as  $m_{c0}$  and  $m_{z0}$ , respectively, after cooling. The wet weight was placed on the electronic scale after weighing  $m_{c1}$  and  $m_{z1}$ , respectively, and the  $m_z$  series specimens were placed into the boiling box; the water level injected into the box was 50 mm higher than the surface of the specimen. After 3 h, heating was stopped and the specimens were cooled to room temperature, with the boiling wet mass being recorded as  $m_{z2}$ . The water absorption rate of the sample brick at room temperature and the 3 h boiling water absorption rate was calculated according to Formulas (4) and (5).

$$W_1 = \frac{m_{c1} - m_{c0}}{m_{c0}} \times 100\% \quad (4)$$

$W_1$ —Water absorption of the sample brick immersed in water at room temperature for 24 h, %.

$m_{c0}$ —Sample brick drying 24 h mass, unit kg.

$m_{c1}$ —Sample brick soaking 24 h mass, unit kg.

$$W_2 = \frac{m_{z2} - m_{z0}}{m_{z0}} \times 100\% \quad (5)$$

$W_2$ —Water absorption of the sample brick by boiling for 3 h, %.

$m_{z0}$ —Sample brick drying mass for 24 h, unit kg.

$m_{z2}$ —Sample brick boiling 3 h mass, unit kg.

### 2.3.3. Frost Resistance Test

The frost resistance of the sintered bricks is one of the important indicators of the durability of the sintered bricks, and also one of the main factors affecting their strength and appearance quality. From the perspective of buildings and structures, the frost resistance of sintered bricks also determines to a large extent the quality, beauty, and the service life of buildings. Freeze–thaw damage to sintered brick can cause internal freezing and cracking, which in turn reduces the load-bearing capacity and stability of the structure. By exploring the appearance changes, mass loss, and dynamic elastic modulus, the laws of external activity and materiality on the performance of sintered bricks are revealed. In this paper, 5 freeze–thaw cycles were used as a cycle. By weighing the mass of sintered brick in each cycle and by conducting strength tests, the mass loss of sintered brick in each freeze–thaw cycle was then calculated.

### 2.3.4. Thermal Analysis

The instrument used was a SDT650 synchronous thermal analyzer from Waters, Milford, MA, USA, with an up-and-down instrument structure and a temperature range of

room temperature to 1500 °C. An appropriate amount of sample was placed in the crucible and detected in an air atmosphere, with a heating rate of 10 °C/min. The information on the thermogravimetric change and the differential heat of the raw material during the heating process was analyzed.

### 2.3.5. Microscopic Morphological Analysis

A HT7700 scanning electron microscope (SEM) from Hitachi, Japan, was used with three observation modes, i.e., low magnification and wide field of view, high contrast observation, and high-resolution observation with a resolution of 0.2 nm and a magnification of up to 600,000 times. The sample is made into a suitable size and representative particle, rinsed on the surface, dried to a constant weight, cooled and glued to the sample stage using conductive tape, sprayed with gold, and then examined.

## 3. Results and Discussions

### 3.1. Influence Law of Compressive Strength

#### 3.1.1. MGB Sintered Brick

(1) Influence of heating rate and holding time on the mechanical properties of sintered brick.

As shown in Figure 3, the mechanical strength of the sintered brick mixed with waste glass slag is improved, which is mainly due to the filling of the micropores of the sintered brick by the glass slag in the high-temperature molten state. When the sintered brick was sintered at a heating rate of 5 °C/min, the strength of the sintered brick reached 10.76 MPa, which was due to the appropriate heating rate to provide sufficient conditions for the volatilization of water vapor, CO<sub>2</sub>, and other gases inside the sintered brick. The mechanical strength reached the maximum value when the heating rate was 10 °C/min. However, with the continuous increase of the heating rate, the strength of the sintered brick started to show a significant decrease.

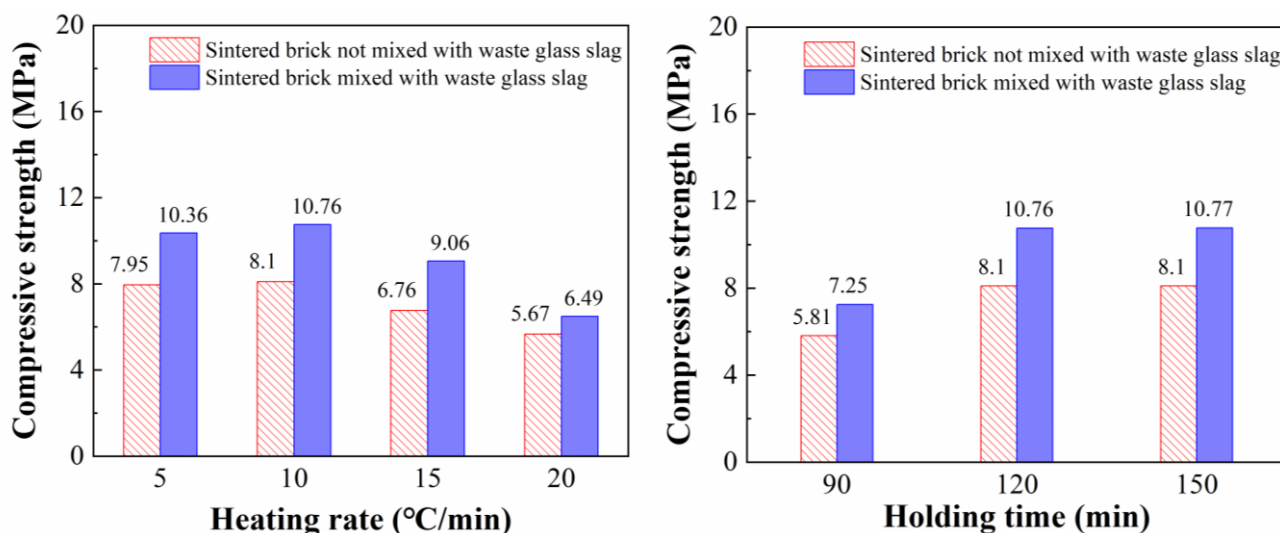


Figure 3. Effect of heating rate and holding time on compressive strength of MGB sintered brick.

As can be seen from Figure 3, when the holding time was 90 min between temperature gradients, the short holding time was not enough to maintain the reaction conditions of the internal physicochemical changes of the sintered brick, and performance indexes such as water absorption rate and the saturation coefficient of the sintered brick did not reach the ideal degree. When the holding time was 120 min and 150 min between the temperature gradients, the physicochemical reaction and heat absorption, and the exothermic process of the sintered brick at high temperature remained stable; the degree of densification of the sintered brick was improved, and the water absorption rate was reduced and kept constant.

Meanwhile, the saturation coefficient was reduced to the minimum value at 120 min of heat preservation. With the incorporation of 10% glass slag, the high-temperature environment showed a significant fluxing effect, and the performance of the sintered brick was further improved. In summary, after fully considering the factors of time, energy consumption, and preparation cost, the test adopted a heating rate and holding time of 10 °C/min and 120 min, respectively.

(2) Effect of sintering temperature on the mechanical properties of sintered brick.

The specimens were sintered in a ZMF-1700C-18L vacuum atmosphere chamber furnace at 950 °C, 1000 °C, 1050 °C, and 1100 °C, respectively.

In this paper, we tested the comparative changes in the mechanical strength of sintered brick made of construction waste and sintered brick prepared by mixing construction waste with waste glass slag under different sintering temperature conditions, as shown in Figure 4. It can be seen from the figure that the strengths of the MRB and MGB sintered bricks reached 8.1 MPa, 8.19 MPa, 10.76 MPa, and 10.79 MPa at 1050 °C and 1100 °C, respectively. The strength of MRB sintered brick was still increasing after 1050 °C, while the strength of the MGB sintered brick did not significantly increase, which is due to the fact that the sintered brick mixed with glass slag was affected by the thermal effect of glass. The sintering temperature was reduced and the thermal stability of the sintered brick under a high-temperature environment was improved. At this stage, the crystallization or rearrangement of the amorphous structure, and the formation of mullite and other material components occurred inside the sintered brick, and the waste glass slag in the molten state combined with the unfused quartz particles to fully fill the tiny cracks inside the sintered brick and enhance the densification degree. With the increase of the maximum sintering temperature, the strength of the sintered brick was not significantly increased.

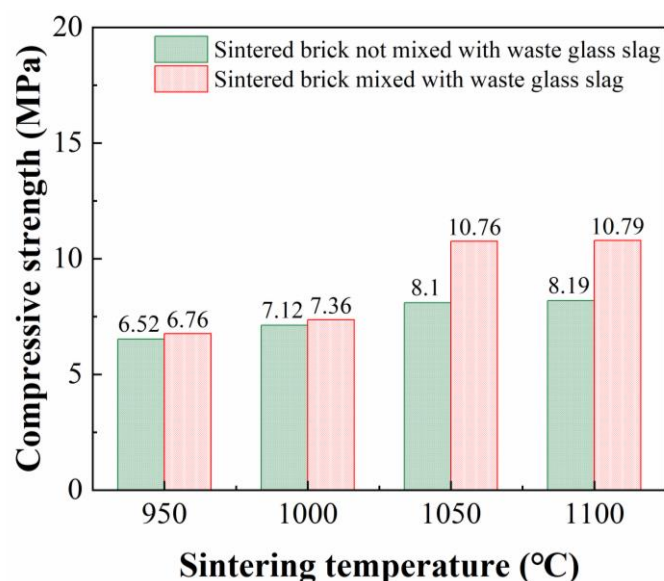


**Figure 4.** Effect of sintering temperature on the compressive strength of the MGB sintered brick.

### 3.1.2. MGS Sintered Brick

(1) Influence law of the heating rate and holding time on the strength of the sintered brick.

From Figure 5, it can be seen that with the increase of the heating rate, the sintered brick strength shows a gentle decreasing trend, which may be due to the adsorption of trace gas between the irregular outer surface of the Yellow River sedimentary sand and the interface of clay particles during the mixing and forming process. The molecular movement of the gas intensifies during the heating process, and the pressure of the gas increases accordingly by the intermolecular impact force. Correspondingly, the surrounding material is affected by the thermal expansion and contraction effect, which also begins to produce additional

stress on the intermediate gas, resulting in a high pressure state of the gas [27]. At this time, the volatile organic compounds are thermally decomposed simultaneously. The bubbles nucleate and expand with an increase in temperature, gradually connecting with the surrounding high-pressure gas to form a connected gas phase. After a brief relief from pressure, it continues to penetrate continuously under pressure along the weakly bound region of the medium to the outside world until the generation of the overflow channel occurs. In this process, an excessive rate of temperature rise will lead to a rapid increase in internal air pressure, resulting in an increase in the number of pores in the sintered brick, and damage to the stability and structure of the brick. In addition, Martin et al. [28] specifically pointed out the presence of lenticular bodies in clay surrounded by sand in their study, and demonstrated that during resistive heating, the lower capillary pressure of the sand, combined with the high temperature near the lenticular bodies, produced gases that led to the agglomeration of these gases at the critical surface between the clay and the sand during the heating of the clay. This result also determines to a large extent the question of the admixture of the sedimentary sand of the Yellow River. Therefore, in contrast, the incorporation of Yellow River sedimentary sand, although it can enrich the skeletal structure inside the sintered brick, also has strict requirements on the heating rate. After experimental analysis, this paper utilized 16% Yellow River sedimentary sand instead of construction waste, and sintered this at a heating rate of 8 °C/min.

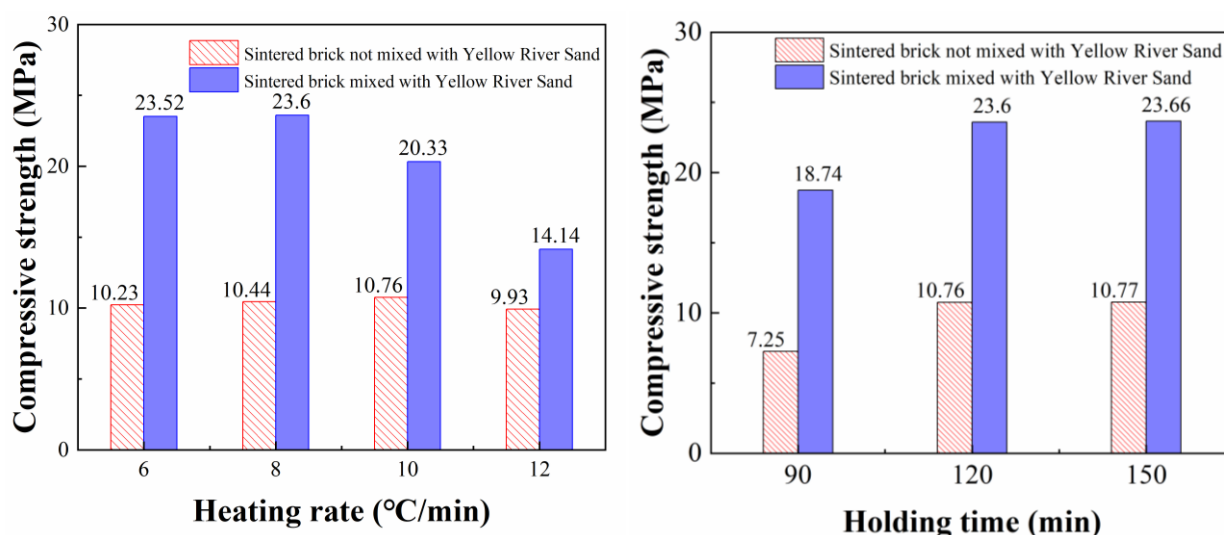


**Figure 5.** Effect of heating rate and holding time on compressive strength of MGS sintered brick.

The effect of heat preservation time on the performance of sintered brick is shown in Figure 5. The effect of holding time on the performance of sintered brick mixed with Yellow River sedimentary sand was not obvious compared with the heating rate, and the strength of sintered brick basically reached the maximum value at the holding time of 120 min. To ensure the uniformity of the experiment, the holding time of the sintered brick mixed with Yellow River sedimentary sand was the same as that of the sintered brick not mixed with Yellow River sedimentary sand.

(2) The effect of sintering temperature on the compressive strength of sintered brick.

The effect of sintering temperature on the compressive strength of sintered brick is shown in Figure 6. Compared with the sintered brick not mixed with Yellow River sedimentary sand, the sintering temperature of the sintered brick increased after mixing with Yellow River sedimentary sand. This is mainly due to the influence of agglomerated gas at the critical surface between clay and sand in the pre-sintering and mid-sintering stages, with gas volatilization leading to an increase of internal pores of the sintered brick; raising the sintering temperature to 1100 °C helped with the formation of the liquid phase of Yellow River sedimentary sand. However, this formation ability gradually decreased

after rising to higher temperatures, and the molten liquid phase filled the internal pores to enhance the densification of the sintered brick body.

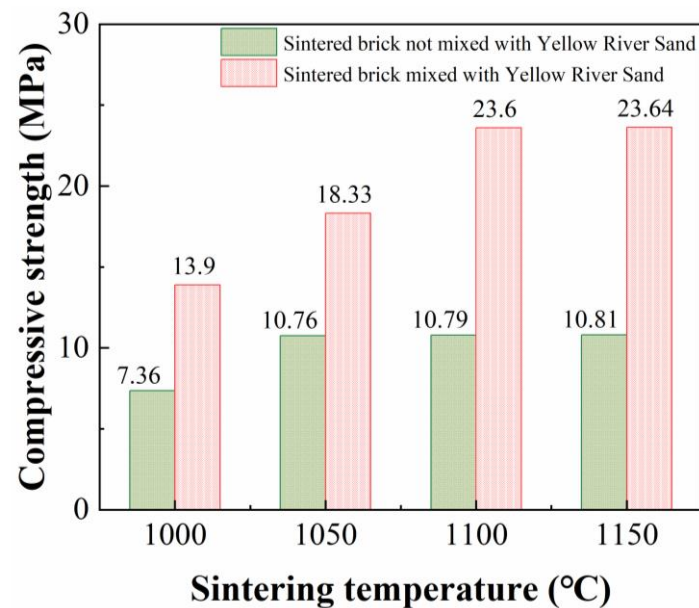


**Figure 6.** Effect of sintering temperature on compressive strength of MGS sintered brick.

Therefore, the internal generation of more morphologically stable gelling products of 16% Yellow River sedimentary sand mixed at 1100 °C can effectively improve the pore structure of the sintered brick and provide better jointing properties at the interface of sand and clay.

### 3.1.3. Microwave Sintered MGS Sintered Brick

(1) Microwave sintering temperature rise rate and holding time on the compressive strength of sintered brick influence law.

In the microwave field, the internal polar molecules of the brick body are synchronously perturbed and resonate with the microwave frequency, which achieves rapid and uniform heating of the billet on a macroscopic scale, resulting in the high quality of the sintered brick. However, due to the high content of free water and bonded water inside the brick body, the excessive heating rate will cause a sharp increase in the pressure difference between the inside and outside of the brick, which eventually leads to the bursting of the brick body. The above problems can be seen in Table 10 and Figure 7a. This paper adopts the interval heating method, with room temperature~300 °C, 300~800 °C, and 800~1050 °C for three intervals; each temperature interval exerts independent control of the heating rate. When the microwave power is low, the highest temperature of the sintered brick interval does not reach the lowest temperature of the next interval, and its heating rate and sintering temperature are not enough to promote the continuous sintering of sintered brick and produce a jumping phenomenon. Different temperature rise types and holding times also have a significant impact on the compressive strength, and sintered brick compressive strength changes, as shown in Figure 7b, with three temperature rise types and different holding times. When the “type 2”, holding time is 30 min, the maximum strength can reach 24.7 MPa, and a heating rate that is too fast or too slow will lead to a significant decrease in the strength of the sintered brick.

**Table 10.** Type of heating rate (°C/min).

Type	Room Temperature—300 °C Range	300~800 °C Range	800~1050 °C Range
1	1.5	3.5	3.9
2	1.9	4.0	4.5
3	2.0	4.5	4.5

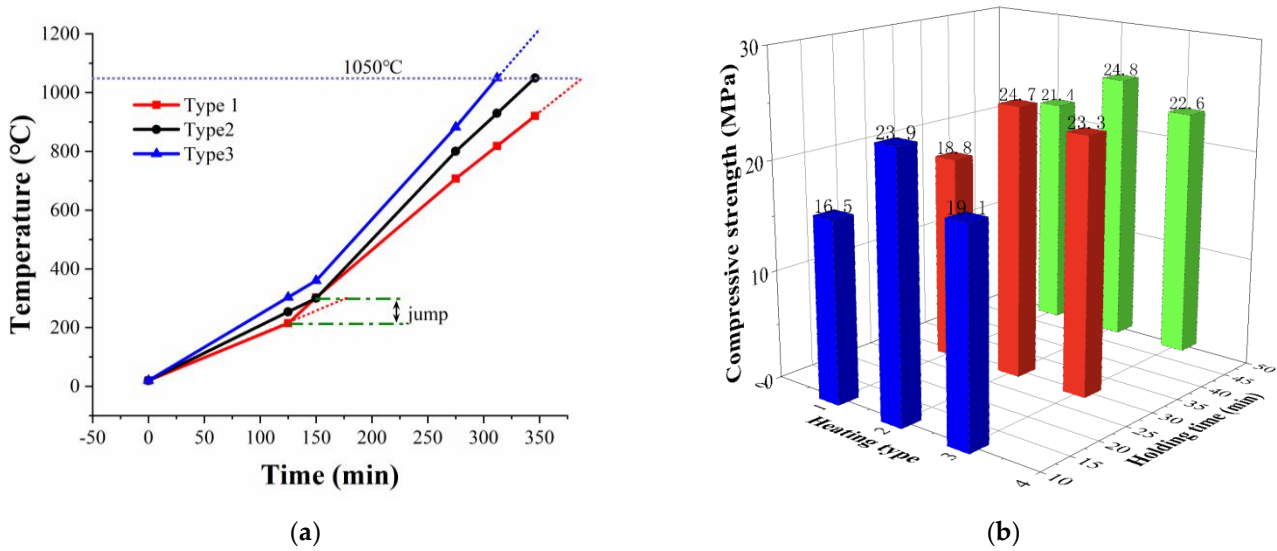


**Figure 7.** Effect of heating rate and holding time on compressive strength of MGS sintered brick. (a) Temperature variation law with time under different heating types. (b) Variation of compressive strength with type of heating.

(2) Effect of microwave sintering temperature on the compressive strength of sintered brick.

From the experimental results of heating sintered brick using an electric furnace process, it is known that the best sintering temperature of the MGS-doped bricks is 1100 °C. However, the sintering temperature of the sintered brick may vary, due to different sintering mechanisms. Therefore, this paper initially chose to investigate the effects of sintering temperatures of 900 °C, 1000 °C, 1050 °C, and 1100 °C on the compressive strength of sintered brick under the conditions of 50% construction waste as the main raw material, 10% waste glass slag, and 16% Yellow River sedimentary sand as admixtures. The results are shown in Figure 8.

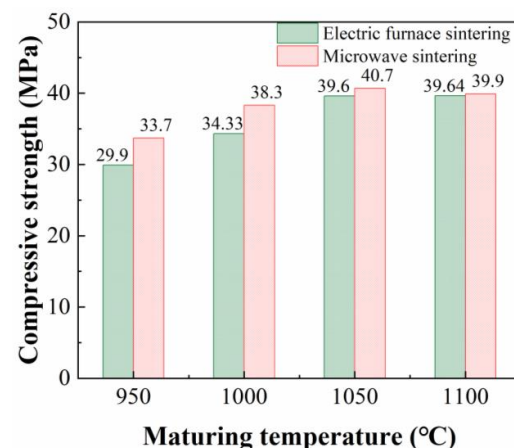


**Figure 8.** Influence of sintering temperature on compressive strength of MGS sintered brick.

As can be seen from Figure 8, with the increase in maturing temperature, the compressive strength of the MGS sintered brick increases, the compressive strength reaches its maximum value when sintered at 1000 °C, and when the maturing temperature reaches 1050 °C and 1100 °C, the strength of the sintered brick changes smoothly without significant growth.

### 3.2. Influence Law of Weathering Resistance

#### 3.2.1. MGB Sintered Brick

(1) Influence of temperature rise rate and holding time on the weathering resistance of sintered brick.

As can be seen from Figure 9, with a temperature rise rate of 5 °C/min and 10 °C/min, the water absorption rate did not change significantly. With an increase in the temperature rise rate, the sintered brick water absorption rate began to significantly increase, which due to the higher temperature rise rate, will lead to an acceleration of the sintered brick water volatilization rate; the limited pore channel has not met the need for water evaporation as brick billets inside a large number of tiny channels that have misconnected or formed external pores, which in turn leads to sintered brick water absorption rate increases. During the sintering process, a series of physical and chemical reactions occur inside the sintered brick. Waste glass slag and other substances become solid-fused during the sintering process, filling the internal pores of the sintered brick and causing the volume of the brick to shrink. At the same time, the internal structure of the brick is destroyed, forming a network structure of interconnected particles, in which the pores are gradually filled and the volume contraction becomes more significant, eventually leading to a reduction in water absorption.

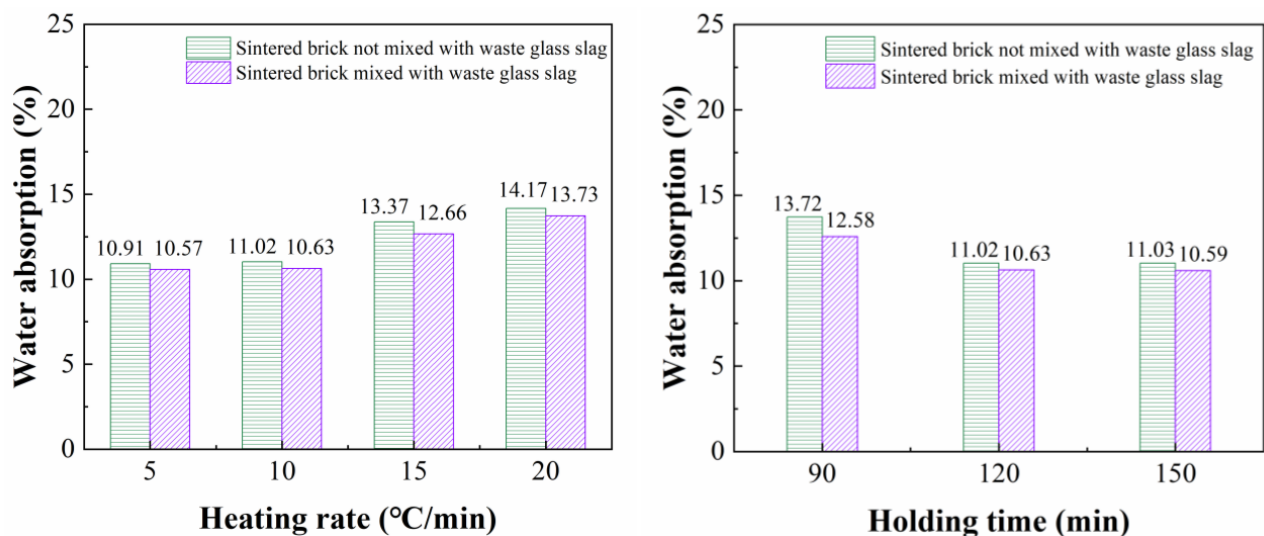


Figure 9. Effect of heating rate and holding time on weathering resistance of MGB sintered brick.

(2) Influence law of sintering temperature on the weathering resistance of sintered brick.

Figure 10 shows the effect law of sintering temperature on the water absorption rate and saturation coefficient of sintered brick. From the figure, it can be seen that the water absorption rate of sintered brick decreases with the increase in sintering temperature. When the sintering temperature was 950 °C, the water absorption rate was 13.56%. When the sintering temperature reached 1050 °C, the water absorption rate and saturation coefficient basically reached the minimum value. As the temperature continued to increase, the water absorption rate and saturation coefficient remained relatively constant. This is because as the sintered brick increases with the sintering temperature, more mineral components inside the brick melt, internal pores and connected pores fill, and the degree of brick densification

increases; when the temperature reaches 1050 °C, the internal physicochemical reaction of the sintered brick basically reaches a stable state.

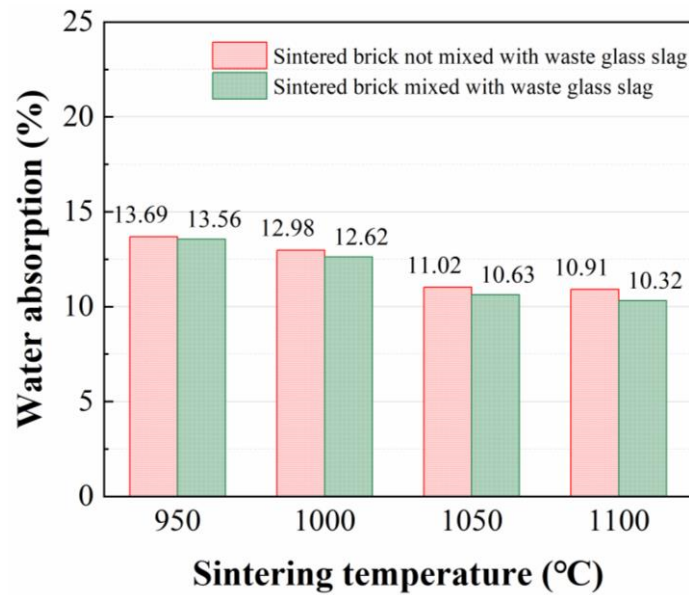


Figure 10. Effect of sintering temperature on water absorption of MGB sintered brick.

### 3.2.2. MGS Sintered Brick

(1) Influence law of temperature rise rate and holding time on the weathering resistance of sintered brick

From Figure 11, it can be seen that when the heating rate is 5 °C/min and 10 °C/min, the evaporation rate of gas inside the sintered brick is weak, and the water absorption rate does not rise significantly; with the increase in heating rate, the water absorption rate of sintered brick starts to increase significantly, which is the same as the reason described in Section 3.1.1. The number of pores and the structure of pores has a direct impact on the water absorption rate of sintered brick; therefore, the heating rate is too large, which will lead to the increase of water absorption rate of sintered brick. In this paper, a temperature rise rate of 8 °C/min and a holding time of 120 min were used for sintering.

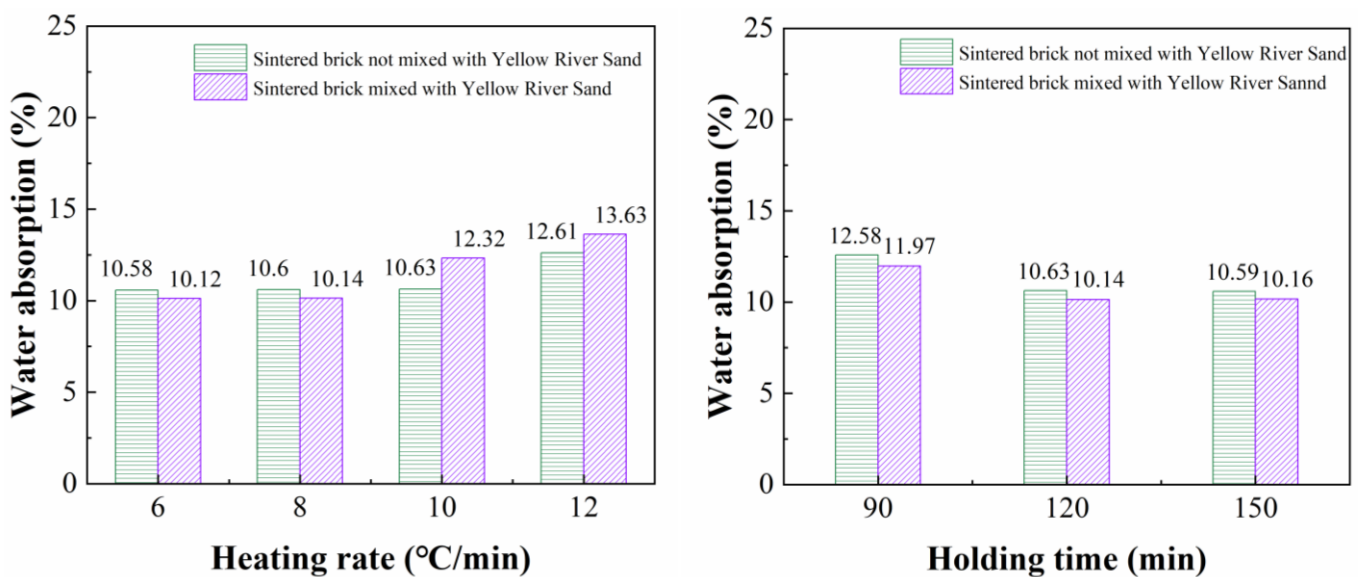


Figure 11. Effect of heating rate and holding time on water absorption of MGS sintered brick.

(2) Influence law of sintering temperature on the weathering resistance of sintered brick.

Figure 12 shows the effect law of sintering temperature on the water absorption rate and saturation coefficient of sintered brick. Obviously, with an increase in sintering temperature, the water absorption rate of sintered brick decreases. When the sintering temperature is 900 °C, the water absorption rate is 17.39%. When the sintering temperature reached 1100 °C, the water absorption rate and saturation coefficient basically reached the minimum value. As the temperature continued to increase, the water absorption rate and saturation coefficient remained relatively constant. This is because with the increase of holding time, more mineral components inside the brick melted, internal pores and connected pores filled, and the degree of brick densification increased, and when the temperature reached 1100 °C, the internal physicochemical reaction of the sintered brick basically reached a stable state.

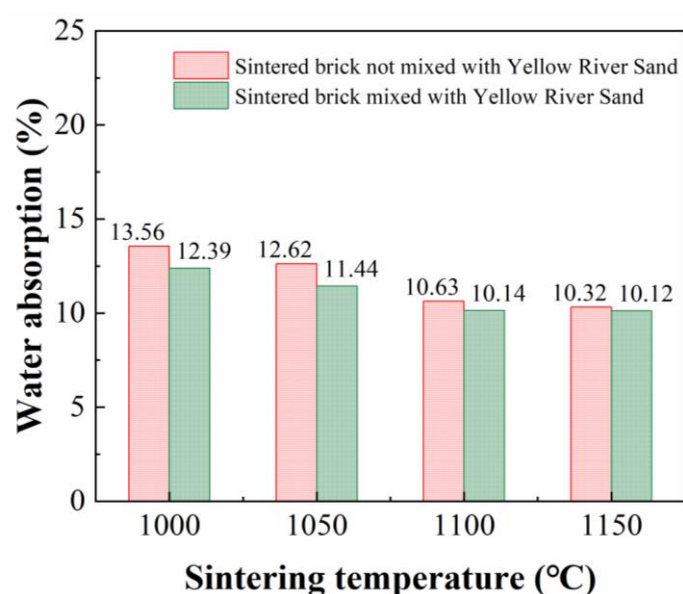


Figure 12. Effect of sintering temperature on water absorption of MGS sintered brick.

### 3.2.3. Microwave Sintering MGS Sintered Brick

(1) Influence of temperature rise rate and heat preservation time on the weathering resistance of MGS sintered brick.

The optimal densification of sintered brick is the balanced result of two opposite trends occurring in the later stages of densification: the sintering capillary force and the pressure of the trapped gas in the closed pores. If the optimal sintering conditions are overcome, expansion may occur, leading to an increase in closed porosity. This is in agreement with the study of Manière et al. [29], where the swelling was observed in conventional sintering under one condition, as shown in Figure 13 and Table 10.

(2) The influence law of sintering temperature on the anti-weathering performance of MGS sintered brick.

It can be seen in Figure 14 that the water absorption rate of sintered brick gradually decreases with an increase in sintering temperature, and the water absorption rate of sintered brick reached the lowest value at the sintering temperature of 1000 °C. This is because a variety of mineral phase changes occur during the sintering process of sintered brick, such as clay dihydroxylation,  $\alpha$ - $\beta$  quartz phase change, mullite formation, glass formation, and feldspar melting, these phase changes lead to changes in the dielectric properties of the material during the sintering process. With an increase in temperature, the tangential loss increases, and materials with a high tangential loss can be easily heated in a microwave environment. It can be seen that the formation of viscous phases and the demand and dependence on the firing temperature of sintered brick sintered in microwave devices are

lower compared to conventional sintering [30]. As the sintering temperature increases, the water absorption of the sintered brick begins to gradually decrease, indicating that the optimal sintering conditions are exceeded at this time, and producing the phenomenon of “over-sintering”. Due to the complexity of the sintered brick composition and phase changes, good control of the sintering process, such as heating rate, holding time, and firing temperature are particularly important for achieving optimal densification, especially in the case of very fast firing cycles. Indeed, this main phase controls the viscous flow of sintering [31] and strongly influences the final properties of the sintered brick.

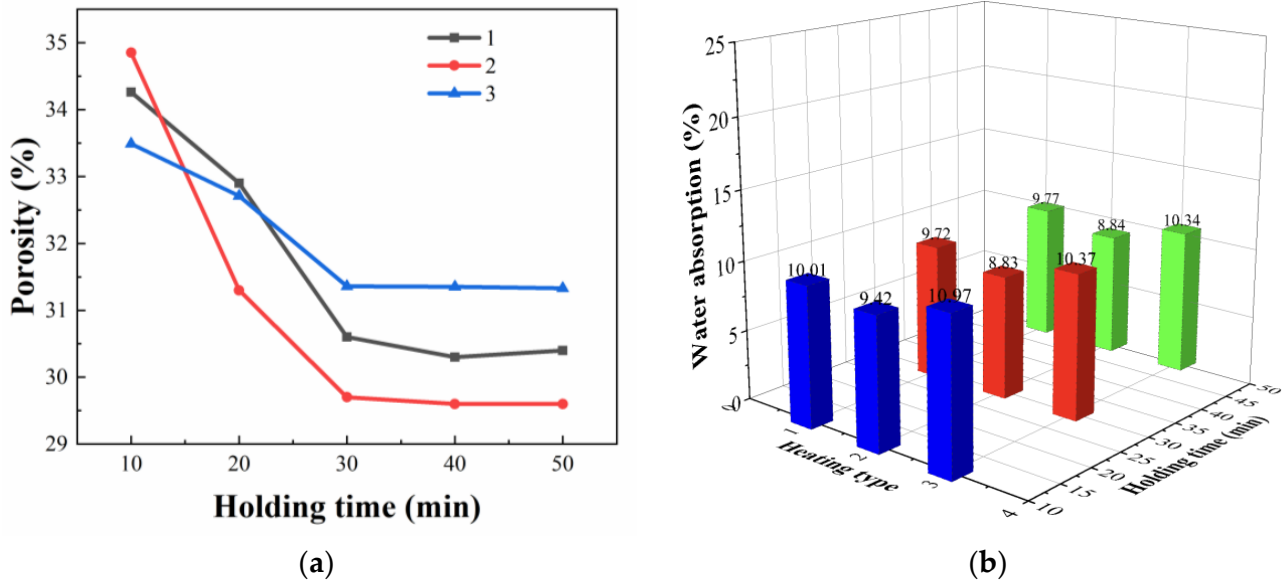


Figure 13. Influence of heating rate and holding time on water absorption of MGS sintered brick. (a) The effect law of heating rate on porosity. (b) The effect of holding time on water absorption rate law.

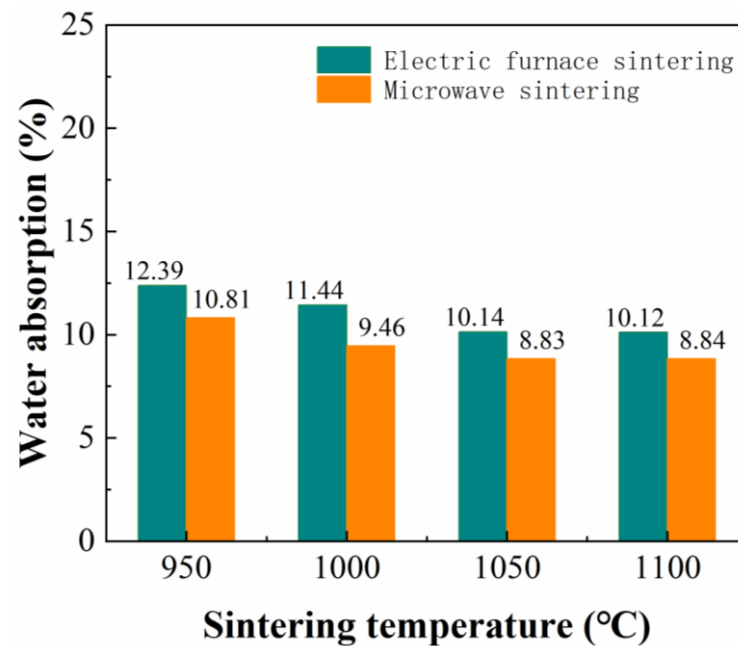
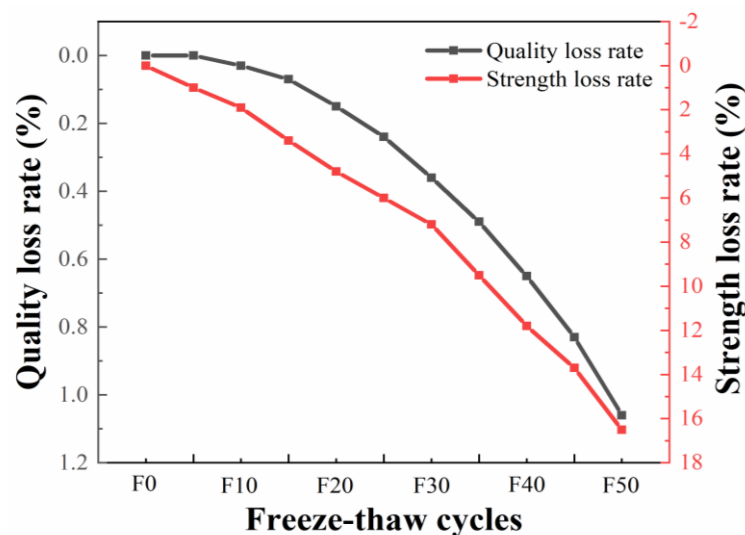


Figure 14. Effect of sintering temperature on water absorption of sintered bricks due to different sintering methods.

### 3.3. Factors Affecting the Frost Resistance of Sintered Brick

#### 3.3.1. MGB Sintered Brick

As shown in Figure 15, it can be seen from the figure that the mass loss rate and strength loss rate of the sintered brick show a trend from slowly decreasing to sharply decreasing with the increase of the number of freeze–thaw cycles, which is due to the cracking of the micropores within the sintered brick in the pre-freeze–thaw period, but with the destruction of the micropore pores by expansion and cracking, the micropore pore size indirectly increases into large micropores. In contrast, large micropores are beneficial for reducing the internal pressure and permeability of the micropores, thus reducing the cracks in the brick structure due to self-shrinkage, and effectively alleviating the stress difference between the ice core and the brick body. Therefore, the appearance of large micropores instead starts to have a beneficial effect on the frost resistance of the material in the direction of reducing the water absorption of the material. However, the large micropores exist only as a stage pore structure, and with the continuous damage by freeze–thaw cycles, the large micropores in the middle and late stages of freeze–thaw gradually change to small pores, and the in situ mesopores and large pores are severely damaged by freeze–thaw, leading to irreversible structural damage of the sintered brick.



**Figure 15.** Quality and strength loss of MGB sintered brick under different freeze–thaw cycles.

#### 3.3.2. MGS Sintered Brick

The effect law of the performance of sintered brick under the action of freeze–thaw cycles is shown in Figure 16, from which it can be seen that in the early stage of freeze–thaw, the quality and strength loss of sintered brick is low, and no obvious change is found in the appearance of the sintered brick, but with the increase of the number of freeze–thaws, the quality and strength loss of the sintered brick starts to rise, and by F50, a large number of cracks appear on the surface of the sintered brick, and the strength of the sintered brick appears significantly reduced.

This is due to the fact that the microcracks inside the Yellow River sedimentary sand will carry trace gas, and after high-temperature sintering, the residual gas will gather numerous tiny spherical bubbles near the micropores. When the pore wall of the micropore ruptures, new microfractures will be created to connect the capillary pore with the nearby bubbles, and the internal water flows into the bubbles through the fractures, and the pressure in the pore space is then reduced. With the increase in the number of freezing and thawing, the nearby bubbles will provide a “pressure relief space” for the capillary pore, eliminating the phenomenon of stress concentration at the tip of the fracture, but this can also play the role of a reservoir to relieve the pore water freezing expansion pressure. Therefore, the appropriate size and distribution of bubble spacing can, to a certain extent,

play a role in improving the frost resistance of sintered brick. However, with the increase in the number of freeze–thaw cycles, this advantage does not exist after the F50 cycle.

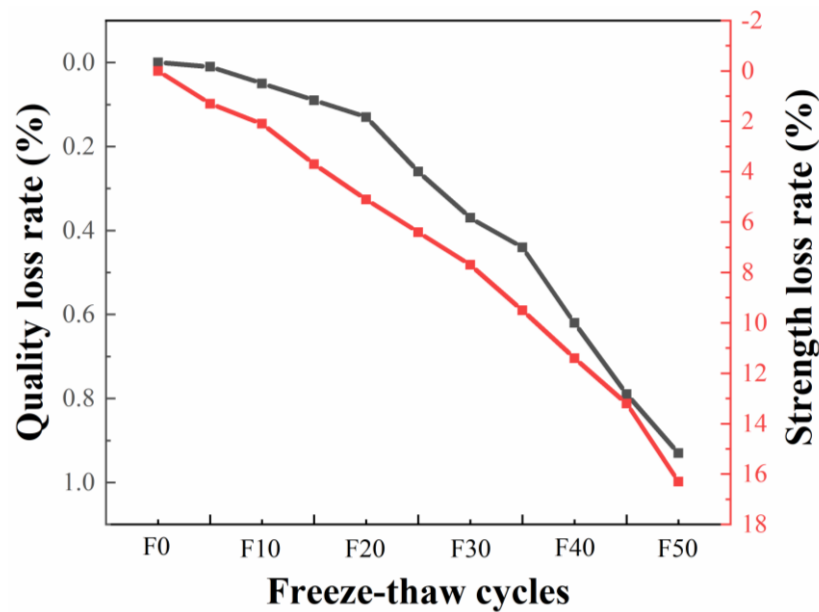


Figure 16. Effect of freeze–thaw cycles on properties of MGS sintered brick.

### 3.3.3. Microwave Sintered MGS Bricks

According to the above experiments, microwave heating can effectively promote the mineral phase change inside the sintered brick, using an increase in the tangential loss of the phase change material to promote the transient and effective microwave heating of the sintered brick, reducing the sintering temperature while improving its densification, and the overall low porosity of the microwave sintered brick compared to the electric furnace sintering. With the increase of the number of freeze–thaw cycles, the percentage of cracks on the outer surface of the sintered brick increases. In this paper, the MGS sintered brick with the best sintering mechanism was selected for comparison tests among the two sintering methods, in which the best porosity of microwave sintered brick and electric furnace sintered bricks were 29.7% and 31.36%, respectively, and the corresponding quality and strength loss rates are shown in Figure 17. It can be seen that microwave sintering has higher denseness than electric furnace sintering.

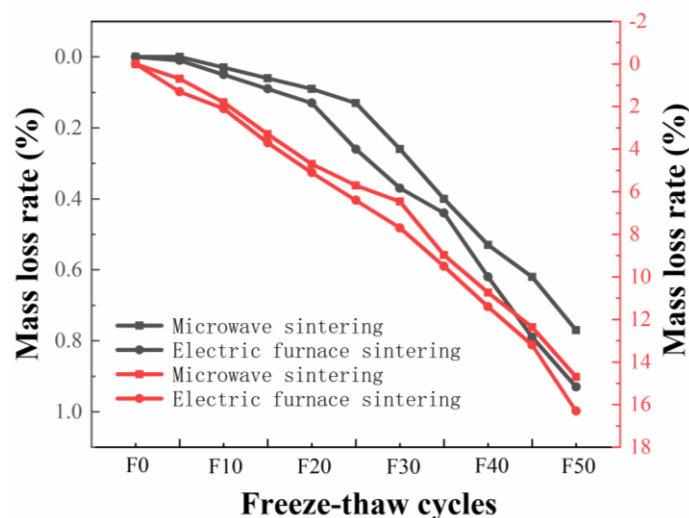


Figure 17. Quality and strength loss rate of recycled brick between two sintering methods.

### 3.4. Thermal Analysis

#### 3.4.1. MGB Sintered Brick

As can be seen from Figure 18, there is a significant weight loss of the mixture at 50~100 °C, when free water starts to evaporate; at 100~550 °C, the combined water evaporates and the mass of the billet decreases smoothly; at 550~700 °C, the organic matter starts to oxidize, and the salts and iron sulfides decompose and oxidize simultaneously, where the stable combined state of C-O and S-O makes it partially decompose into  $\text{CO}^{2+}\text{O}^{2-}$ ,  $\text{SO}^{2+}\text{O}^{2-}$  and  $\text{O}^{2-}$  combined with cations to generate new substances produce gases such as  $\text{CO}_2$ ,  $\text{SO}_2$ , and  $\text{SO}_3$ , and gas volatilization leads to a sharp decline in the quality of the mixture; this stage of insulation treatment can stabilize the rate of gas volatilization and reduce the porosity; at around 700 °C, new substances are generated within the billet. After 950 °C, the liquid phase is formed, the lattice is completely disintegrated, and the active oxides form new minerals. Based on the above thermogravimetric analysis results, five temperature gradients of sintered bricks were set from 0 to 300 °C, 300 to 500 °C, 500 to 900 °C, and 900 to 1050 °C, and each of the two gradients were insulated for 2 h. The internal reflections of sintered bricks at different temperatures are shown in Figure 19.

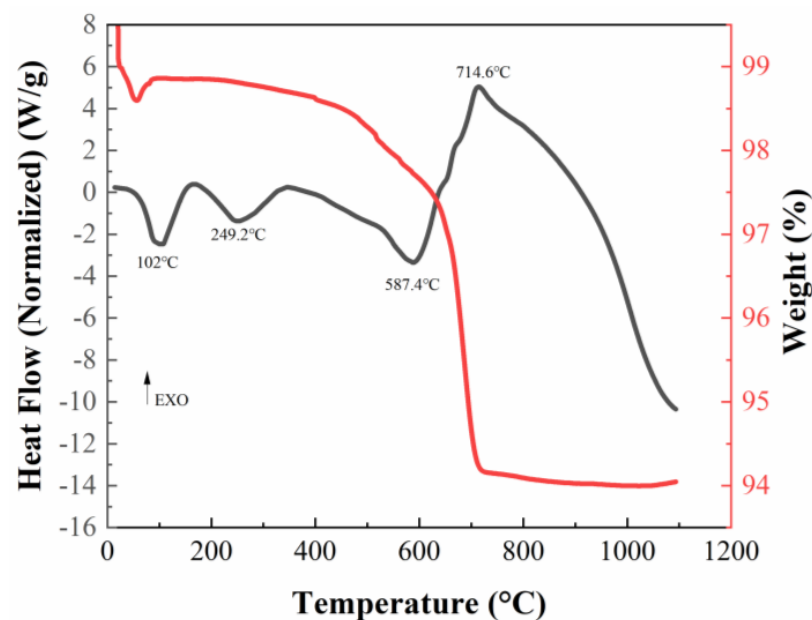


Figure 18. DSC–TG curve of mixture of MGB Sintered Brick.

#### 3.4.2. MGS Sintered Brick

It can be seen from Figure 20 that when heated from room temperature to 200 °C, the sintered brick produces an obvious weight loss, which is caused by the evaporation of free water and bound water; at 400–700 °C, the sintered brick produces weight loss, which is attributed to the dehydroxylation of clay (i.e., the transformation of kaolinite into metakaolinite and the decomposition of chemically bound water), the clay undergoes a dihydroxylation phase change and quartz produces  $\alpha$ - $\beta$  quartz phase change; no significant mass loss was seen at temperatures greater than 700 °C; an insignificant exothermic peak was observed at 900 °C, which was related to the formation of mullite from metakaolinite. The DSC curves of the mixture were generally smooth, with no obvious heat absorption or exothermic peaks, indicating that the mixture was relatively stable in the air under high-temperature conditions.

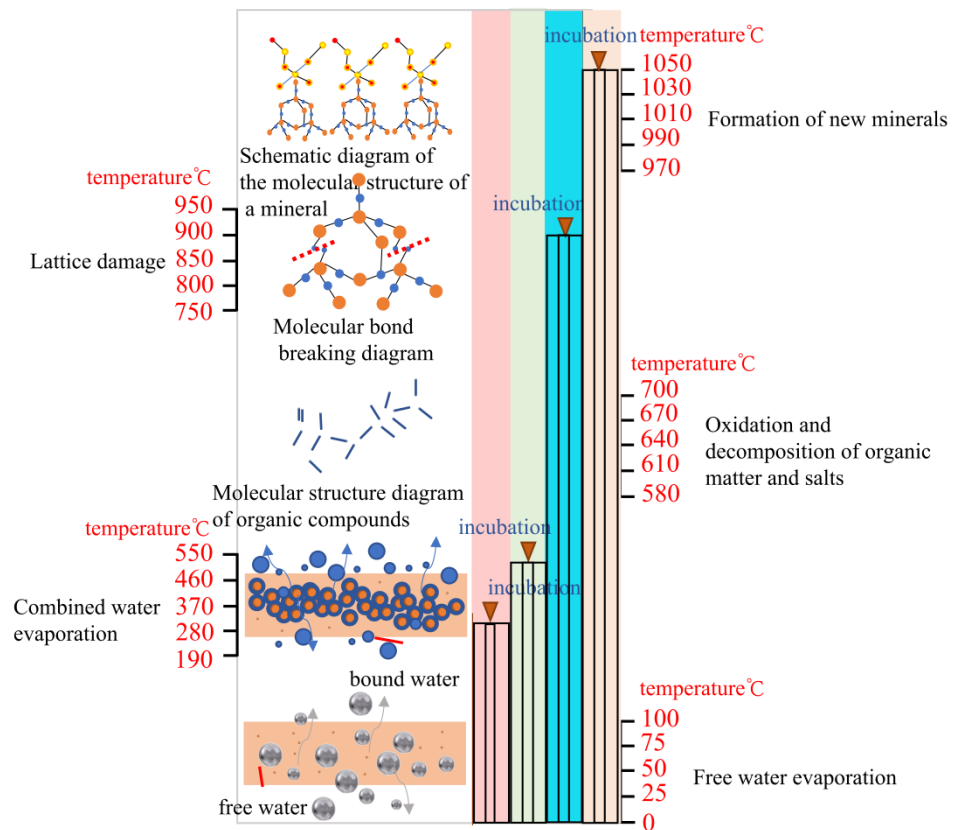


Figure 19. Internal reflection of recycled brick at different temperatures.

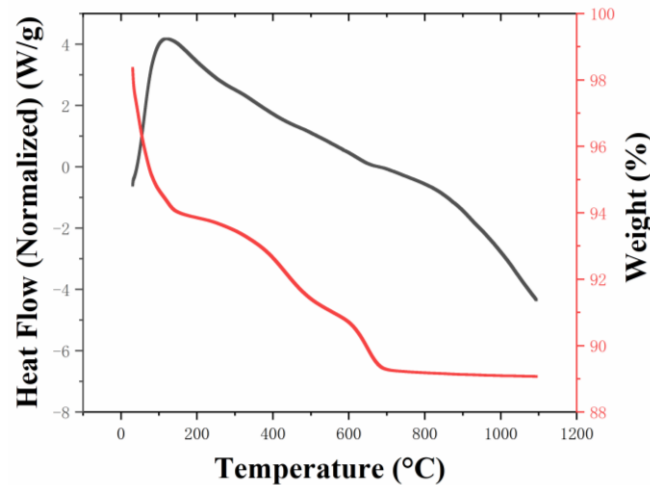


Figure 20. DSC–TG curve of mixture of MGS Sintered Brick.

### 3.5. Microscopic Morphological Analysis

#### 3.5.1. MGB Sintered Brick

Combined with the XRD of the sintered brick in Figure 21, it can be seen that the MGB sintered brick has quartz ( $\text{SiO}_2$ ) as the main material phase. A comparison of the SEM microscopic morphology of construction for waste sintered brick before and after mixing with glass slag is shown in Figure 22a,b. Most of the micropores of construction waste sintered bricks not mixed with waste glass slag are uniformly distributed in a circular shape. Its water vapor overflows uniformly along all directions during sintering, which reduces the environmental pressure difference between the inside and the outside of the brick, making the brick less likely to produce cracking. However, the limited high-temperature liquid phase in the late sintering period cannot fill too many pores, resulting in the excessive

water absorption of sintered bricks and reduced mechanical properties. The sintered brick mixed with waste glass slag is accompanied by the production of a large amount of high-temperature liquid phase in the late sintering stage, which greatly seals the micropores formed by calcite transformation. The large amount of high-temperature liquid phase wraps and enhances the degree of bonding between the particles, which improves the quality of the sintered brick by forming a glass phase after sintering is completed and the brick is cooling.

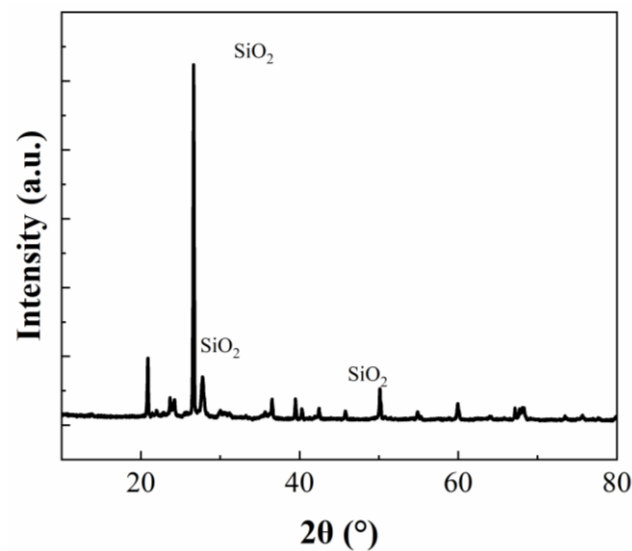


Figure 21. XRD analysis of MGB sintered brick.

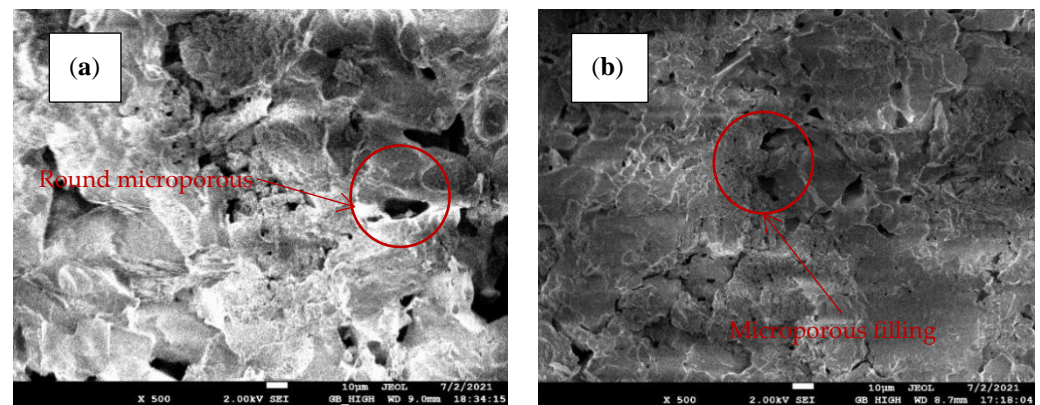


Figure 22. Comparison of SEM micromorphology of two kinds of sintered bricks. (a) MRB sintered brick. (b) MGB sintered brick.

For example, a higher sintering rate will lead to an increase in the fractal dimension of the pores and a more complex structure, which will inhibit the frost resistance of the sintered brick. Conversely, higher sintering temperatures can lead to higher vitrification and a relatively lower porosity of the sintered brick, thus improving the frost resistance. Therefore, this paper analyzes the variation of pore structure in conjunction with SEM microscopic images, and also simultaneously investigates the degree of influence of the sintering rate and the firing temperature on the performance of the sintered brick.

### 3.5.2. MGS Sintered Brick

The crystal mineral composition of MGS sintered brick prepared under optimal conditions was analyzed and determined using an X-ray diffractometer, and the results are shown in Figure 23. From the figure, it can be seen that the main components of MGS

sintered bricks are:  $\text{SiO}_2$ , sodium feldspar ( $\text{Na}(\text{Si}_3\text{Al})\text{O}_8$ ,  $\text{Na}(\text{AlSi}_3\text{O}_8)$ ), calcium feldspar ( $\text{CaAl}_2\text{Si}_2\text{O}_8$ ), and hematite ( $\text{Fe}_2\text{O}_3$ ), and a small amount of  $\text{Al}_2\text{SiO}_5$ . A comparison with the X-ray diffractograms of the raw materials shows that the content of calcium feldspar increases after high-temperature sintering, causing the disappearance of acanthite and calcite, while hematite appears as a new mineral component. This indicates that calcite and plagioclase zeolite decompose at high temperature, where the decomposition product of calcite,  $\text{CaO}$ , is again involved in the generation of calcium feldspar. The decomposition of iron phosphate forms hematite, and the decomposition of illite participates in the generation of erythrite. In short, the unstable or poorly thermally stable components of the raw material are gradually transformed into other new mineral components with excellent thermal stabilities.

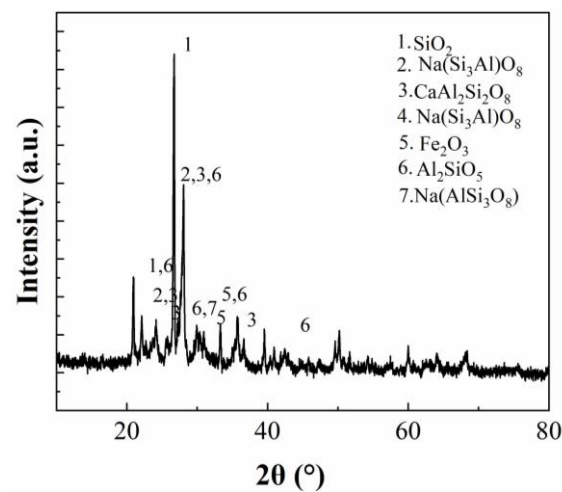


Figure 23. XRD analysis of MGS recycled brick.

The SEM of sintered brick is shown in Figure 24. When sintering at high temperatures, the lattice of salt and other compound components within the brick is broken and reorganized, the oxides are recrystallized, and the glass phase is formed after cooling of the high-temperature liquid phase appears inside. Part of the glass phase wraps and bonds the grains to form a solid solution phase, which reduces the porosity of the brick, thus ensuring the strength of the brick and reducing the water absorption rate. In addition, the new mullite crystalline phase is a binary compound with low creep value at high temperature, high hardness, and a uniform and stable expansion. The new crystalline phase mullite and other main crystalline phases form the sintered brick skeleton, which effectively improves the structural stability and mechanical properties of the sintered brick.

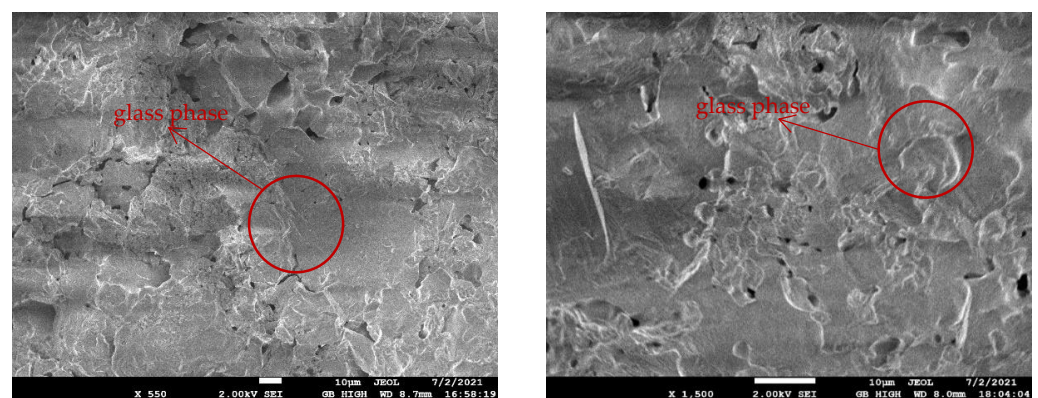


Figure 24. SEM micromorphology of MGS sintered brick.

### 3.5.3. Microwave Firing of MGS Sintered Brick

Figure 25 shows the SEM micrographs of the MGS sintered brick, from which it can be seen that pores of different sizes and shapes are observed in the permeable region, which indicates a dense microstructure with a small number of pores between the grains. In the microwave field, in addition to the formation of alternating phase reaction layers between the clay minerals and the material in the Yellow River sedimentary sand, the viscosity of the glassy melt is also decreasing with increasing temperature, and the molten liquid phase penetrates along the grain boundaries and pores or voids, which in turn enhances the overall denseness of the sintered brick. In the later stages of sintering, mullite, quartz, and glassy amorphous phases, as well as rhodochrosite gradually form, and the strength of the sintered brick increases. In addition, Wiesner et al. [32] found that other trace oxides present in the melt, including iron and potassium oxides, may greatly affect the high-temperature viscosity of the melt, but do not lead to the formation of alternate phases, and the combination of the XRF analysis results of the Yellow River sedimentary sand and the microscopic images of the sintered brick doped with Yellow River sedimentary sand show that the doping of the Yellow River sedimentary sand largely promotes this state in the sintered brick. The degree of compliance of the sintered brick with this condition was largely facilitated by the incorporation of Yellow River sedimentary sand. The use of microwave sintering promotes the densification, homogenization, and integrity of sintered brick compared to electric furnaces.

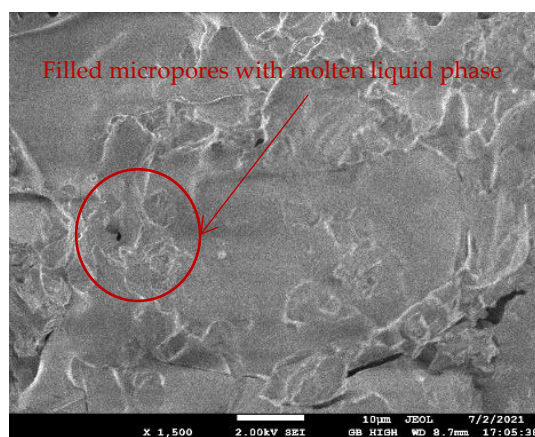


Figure 25. SEM microscopic morphology of MGS sintered bricks prepared by microwave process.

## 4. Conclusions

In this paper, a combination of theoretical analysis and experimental tests was used to analyze the basic physical properties and chemical compositions of three solid wastes, namely, construction waste, waste glass slag, and Yellow River sedimentary sand as the test raw materials. Exploring the influence law of the sintering mechanism on the mechanical properties, weathering resistance, and frost resistance of sintered brick, the following conclusions were drawn.

(1) The amount of construction waste plays a crucial role in the strength of sintered brick. When the amount of construction waste is 50%, it can play its cohesive role and make the sintered brick have a good performance. However, when the amount of construction waste reaches 55% or even higher, it will lead to the reduction of other admixtures of sintered brick and inhibit the strength of the sintered brick.

(2) After adding Yellow River sedimentary sand, the mechanical properties of sintered brick are improved from 10.76 MPa to 23.6 MPa, the content of trace elements such as iron and potassium oxides are reduced, and the performance is improved, but there are also strict requirements on the heating rate. The heating rate and maximum temperature increased with the increase of the content of Yellow River sedimentary sand in the sintered brick, and produced gas at the sand–soil interface around the lenticular body. When the

doping amount is greater than 16%, a large amount of gas leads to the destruction of structure and stability during the sintering of sintered brick.

(3) The 10% waste glass slag can play a fluxing effect on the sintered brick, reducing energy consumption and shortening the sintering time at the same time. In addition, 10% of waste glass slag can form a liquid phase in a high-temperature environment, which improves the SiO<sub>2</sub> composition in the mixture, solves the problem of the gas chamber and overflow channel formed by the gas generated by Yellow River sedimentary sand in a high-temperature environment, and enhances the densification of the sintered brick.

(4) In the process of sintering using a vacuum atmosphere chamber furnace, heat is radiated from the heating element to the whole furnace chamber and the external environment of the sintered brick is stable, but the temperature penetration rate is poor, and the sintering time is nearly 12 h. In addition, because the electric furnace adopts radiation heating, the outer hard layer appears on the outer surface of the sintered brick, preferentially in the early stage of heating, resulting in the slow evaporation of internal gas, and the heating rate is 10 °C/min.

(5) The use of a microwave sintering high-temperature furnace for heating can realize the monolithic sintering of sintered brick, and the interaction between polar molecules in the microwave field can accelerate the promotion of a phase change transformation of the internal mineral composition of sintered brick, leading to changes in the dielectric properties of the material during the sintering process to achieve a higher heating performance of sintered brick. Compared with radiation heating, microwave heating can improve the sintering time by 43.6% while maintaining the best performance of the sample.

**Author Contributions:** Conceptualization, H.Q. and C.G.; methodology, C.G.; software, Z.W.; formal analysis, J.K. and W.W.; investigation, C.G.; resources, H.Q.; data curation, Z.W., X.M. and Y.Z.; writing—original draft preparation, C.G.; writing—review and editing, C.G., J.K., W.W. and H.Q.; visualization, X.M. and Y.Z.; supervision, H.Q.; project administration, H.Q.; funding acquisition, H.Q. All authors have read and agreed to the published version of the manuscript.

**Funding:** This research was funded by [the Natural Science Foundation of Shandong Province] grant number [ZR2021ME110].

**Acknowledgments:** This work was supported by the Natural Science Foundation of Shandong Province [grant number ZR2021ME110].

**Conflicts of Interest:** The authors declare no conflict of interest.

## References

1. Laurent, A.; Bakas, I.; Clavreul, J.; Bernstad, A.; Niero, M.; Gentil, E.; Hauschild, M.Z.; Christensen, T.H. Review of LCA studies of solid waste management systems—Part I: Lessons learned and perspectives. *Waste Manag.* **2014**, *34*, 573588. [[CrossRef](#)] [[PubMed](#)]
2. Long, W.-J.; Peng, J.-K.; Gu, Y.-C.; Li, J.-L.; Dong, B.; Xing, F.; Fang, Y. Recycled use of municipal solid waste incinerator fly ash and ferronickel slag for eco-friendly mortar through geopolymers technology. *J. Clean. Prod.* **2021**, *307*, 127281. [[CrossRef](#)]
3. Le, L.; Xinghua, F.; Wenhong, T.; Chunxia, Y.; Mengchao, M. Research on the preparation of new lightweight wall materials from construction residues. *Guangdong Build. Mater.* **2021**, *37*, 912.
4. Hao, Z. Method for Modifying Mixed Construction Muck and Surplus Sludge Based on Microbial Induced Carbonate Precipitation (MICP). Master's Thesis, Zhejiang Sci-Tech University, Hangzhou, China, 2020.
5. Chuang, Z. Application of construction debris in municipal road foundation project. *Glob. Mark.* **2021**, *15*, 314316.
6. Zhao, C.; Zhao, D. Application of construction waste in the reinforcement of soft soil foundation in coastal cities. *Environ. Technol. Innov.* **2021**, *21*, 101195. [[CrossRef](#)]
7. Ling, Z. Study on Preparation and Properties of New-type Sintered Bricks by Construction Wastes and Industrial Residues. Master's Thesis, Zhengzhou University, Zhengzhou, China, 2019.
8. Xiaojuan, D.; Haifeng, Y.; Jiaqi, L. Feasibility study of using construction residue to produce new sintered wall materials. *Brick Tile World* **2016**, 50–52.
9. Chen, Z.; Wang, Y.; Liao, S.; Huang, Y. Grinding kinetics of waste glass powder and its composite effect as pozzolanic admixture in cement concrete. *Constr. Build. Mater.* **2020**, *239*, 117876. [[CrossRef](#)]
10. Sun, J.; Tang, Y.; Wang, J.; Wang, X.; Wang, J.; Yu, Z.; Cheng, Q.; Wang, Y. A multi-objective optimisation approach for activity excitation of waste glass mortar. *Mater. Res. Technol.* **2022**, *17*, 22802304. [[CrossRef](#)]

11. Song, H.; Chai, C.; Zhao, Z.; Wei, L.; Wu, H.; Cheng, F. Experimental study on foam glass prepared by hydrothermal hot pressing-calcination technique using waste glass and fly ash. *Ceram. Int.* **2021**, *47*, 2860328613. [[CrossRef](#)]
12. An, C.; Lu, J.; Qian, Y.; Wu, M.; Xiong, D. The scour-deposition characteristics of sediment fractions in desert aggrading rivers—taking the upper reaches of the Yellow River as an example. *Quat. Int.* **2019**, *523*, 5466. [[CrossRef](#)]
13. Bai, T.; Wei, J.; Chang, F.; Yang, W.; Huang, Q. Optimize multi-objective transformation rules of water-sediment regulation for cascade reservoirs in the Upper Yellow River of China. *J. Hydrol.* **2019**, *577*, 123987. [[CrossRef](#)]
14. Guo, W.; Xi, B.; Huang, C.; Li, J.; Tang, Z.; Li, W.; Ma, C.; Wu, W. Solid waste management in China: Policy and driving factors in 2004–2019. *Resour. Conserv. Recycl.* **2021**, *173*, 105727. [[CrossRef](#)]
15. Chen, Y.; Du, W.; Zhuo, S.; Liu, W.; Liu, Y.; Shen, G.; Wu, S.; Li, J.; Zhou, B.; Wang, G.; et al. Stack and fugitive emissions of major air pollutants from typical brick kilns in China. *Environ. Pollut.* **2017**, *224*, 421429. [[CrossRef](#)] [[PubMed](#)]
16. Ying, Y.; Ma, Y.; Li, X.; Lin, X. Emission and migration of PCDD/Fs and major air pollutants from co-processing of sewage sludge in brick kiln. *Chemosphere* **2021**, *265*, 129120. [[CrossRef](#)] [[PubMed](#)]
17. Xiao, J.; Shen, J.; Bai, M.; Gao, Q.; Wu, Y. Reuse of construction spoil in China: Current status and future opportunities. *J. Clean. Prod.* **2021**, *290*, 125742. [[CrossRef](#)]
18. Ma, W.; Hoo, S.-B. Preparation of sintered bricks using municipal sludge as admixture. *J. Environ. Eng.* **2012**, *06*, 10351038.
19. Sun, J.; Zhou, H.; Jiang, H.; Zhang, W.; Mao, L. Recycling municipal solid waste incineration fly ash in fired bricks: An evaluation of physical-mechanical and environmental properties. *Constr. Build. Mater.* **2021**, *294*, 123476. [[CrossRef](#)]
20. Dubale, M.; Goel, G.; Kalamdhad, A.; Singh, L.B. An investigation of demolished floor and wall ceramic tile waste utilization in fired brick production. *Environ. Technol. Innov.* **2022**, *25*, 102228. [[CrossRef](#)]
21. Erdogmus, E.; Harja, M.; Gencel, O.; Sutcu, M.; Yaras, A. New construction materials synthesized from water treatment sludge and fired clay brick wastes. *J. Build. Eng.* **2021**, *42*, 102471. [[CrossRef](#)]
22. Wang, T.; Nicolas, R.S.; Kashani, A.; Ngo, T. Sustainable utilisation of low-grade and contaminated waste glass fines as a partial sand replacement in structural concrete. *Case Stud. Constr. Mater.* **2022**, *16*, e00794. [[CrossRef](#)]
23. Cheng, M.; Chen, M.; Wu, S.; Yang, T.; Zhang, J.; Zhao, Y. Effect of waste glass aggregate on performance of asphalt micro-surfacing. *Constr. Build. Mater.* **2021**, *307*, 125133. [[CrossRef](#)]
24. Fu, C.; Liang, J.; Yang, G.; Dagestani, A.a.; Liu, W.; Luo, X.; Zeng, B.; Wu, H.; Huang, M.; Lin, L.; et al. Recycling of waste glass as raw materials for the preparation of self-cleaning, light-weight and high-strength porous ceramics. *J. Clean. Prod.* **2021**, *317*, 128395. [[CrossRef](#)]
25. Chen, M.; Li, J.; Xie, Y.; Shi, K.; Zhu, A.; Chen, G.; Li, X.; Liu, Y. A novel  $\text{Sr}_2\text{Nd}_8(\text{SiO}_4)_6\text{O}_2$  glass-ceramics for rapid immobilization of FP and  $\text{An}^{3+}$  co-doped uranium tailings by microwave sintering: Mechanism and performance. *J. Nucl. Mater.* **2022**, *563*, 153640. [[CrossRef](#)]
26. GB/T 2542-2012; Test Methods for Masonry Wall Bricks. Ministry of Housing and Urban-Rural Development of the People's Republic of China: Beijing, China; China Quality Inspection Press: Qingdao, China; China Standard Press: Beijing, China, 2012.
27. Martin, E.J.; Mumford, K.G.; Kueper, B.H.; Siemens, G.A. Gas formation in sand and clay during electrical resistance heating. *Int. J. Heat Mass Transf.* **2017**, *110*, 855862. [[CrossRef](#)]
28. Martin, E.J.; Mumford, K.G.; Kueper, B.H. Electrical Resistance Heating of Clay Layers in Water-Saturated Sand. *Groundw. Monit. Remediat.* **2016**, *36*, 5461. [[CrossRef](#)]
29. Manière, C.; Harnois, C.; Marinel, S. 3D printing of porcelain and finite element simulation of sintering affected by final stage pore gas pressure. *Mater. Today Commun.* **2021**, *26*, 102063. [[CrossRef](#)]
30. Lerdprom, W.; Zapata-Solvas, E.; Jayaseelan, D.D.; Borrell, A.; Salvador, M.D.; Lee, W.E. Impact of microwave processing on porcelain microstructure. *Ceram. Int.* **2017**, *43*, 1376513771. [[CrossRef](#)]
31. Conte, S.; Zanelli, C.; Ardit, M.; Cruciani, G.; Dondi, M. Phase evolution during reactive sintering by viscous flow: Disclosing the inner workings in porcelain stoneware firing. *Eur. Ceram. Soc.* **2020**, *40*, 17381752. [[CrossRef](#)]
32. Wiesner, V.L.; Harder, B.J.; Bansal, N.P. High-Temperature Interactions of Desert Sand CMAS Glass with Yttrium Disilicate Environmental Barrier Coating Material. *Ceram. Int.* **2018**, *44*, 2273822743. [[CrossRef](#)]